Chapter 4
Characterization Methods of Encapsulates

Zhibing Zhang, Daniel Law, and Guoping Lian

4.1 Introduction

Food active ingredients can be encapsulated by different processes, including spray drying, spray cooling, spray chilling, spinning disc and centrifugal co-extrusion, extrusion, fluidized bed coating and coacervation (see Chap. 2 of this book). The purpose of encapsulation is often to stabilize an active ingredient, control its release rate and/or convert a liquid formulation into a solid which is easier to handle. A range of edible materials can be used as shell materials of encapsulates, including polysaccharides, fats, waxes and proteins (see Chap. 3 of this book). Encapsulates for typical industrial applications can vary from several microns to several millimetres in diameter although there is an increasing interest in preparing nano-encapsulates. Encapsulates are basically particles with a core-shell structure, but some of them can have a more complex structure, e.g. in a form of multiple cores embedded in a matrix. Particles have physical, mechanical and structural properties, including particle size, size distribution, morphology, surface charge, wall thickness, mechanical strength, glass transition temperature, degree of crystallinity, flowability and permeability. Information about the properties of encapsulates is very important to understanding their behaviours in different environments, including their manufacturing processes and end-user applications. E.g. encapsulates for most industrial applications should have desirable mechanical strength, which should be strong enough to withstand various mechanical forces generated in manufacturing processes, such as mixing, pumping, extrusion, etc., and may be required to be weak enough in order to release the encapsulated active ingredients by mechanical forces at their end-user applications, such as release rate of flavour by chewing. The mechanical strength of encapsulates and release rate of their food actives are related

Z. Zhang (✉) and D. Law
School of Chemical Engineering, University of Birmingham, Edgbaston, Birmingham, B15 2TT, UK
e-mail: z.zhang@bham.ac.uk

G. Lian
Unilever Discover, Colworth, Shanrnbrook, Bedford, MK44 1LQ, UK

N.J. Zuidam and V.A. Nedović (eds.), *Encapsulation Technologies for Active Food Ingredients and Food Processing*,
DOI 10.1007/978-1-4419-1008-0_4,

to their size, morphology, wall thickness, chemical composition, structure etc. Hence, reliable methods which can be used to characterize these properties of encapsulates are vital. In this chapter, the state-of-art of these methods, their principles and applications, and release mechanisms are described as follows.

4.2 Physical Characterization Techniques

4.2.1 Characterization by Microscopy, X-ray and Laser Light Scattering

Physical properties of encapsulates include their size, size distribution, shape, morphology and surface charge, which can be measured by commercially available instruments based on principles of microscopy, X-ray and laser light scattering.

4.2.1.1 Microscopy

Optical and electron microscopy have been widely used to provide important information about size, surface topography, shell thickness and sometimes porosity of the shell material of encapsulates in food product. The performance and dissolution properties of encapsulates with active ingredients are often related to the physical properties.

Conventional Optical Microscopy

A standard upright optical microscope is capable of characterising structures that are 0.2 μm or greater as restricted by the wavelength of light. Often digital images or video images of a specimen are taken, followed by quantitative analysis using image analysis software. The size of single encapsulates can be measured. If encapsulates are not spherical, their shape may be characterized by a shape parameter circularity, which is sometimes called "roundness (RN)", and corresponds to a minimum value of unity for a circle. It is defined by the following equation:

$$RN = P^2 / (4\pi A) \tag{4.1}$$

where P is the perimeter of single encapsulates and A is their cross-sectional area.

Confocal Laser Scanning Microscopy

Confocal Laser Scanning Microscopy (CLSM) can be used to produce in-focus images of a fluorescent specimen by optical sectioning. The fluorescent specimen is illuminated by a point laser source, and each volume element of the specimen is

associated with discrete fluorescence intensity. Images of a thick object can be obtained point-by-point and its three-dimensional structure can be reconstructed with a computer software package. For example, gelatin and gum arabic have been used to encapsulate an oil-based active ingredient by a complex coacervation process. The polymers were labelled with fluorescent markers. The spatial distribution of both gelatin and arabic gum throughout the encapsulate shell was identified by CLSM (Lamprecht et al. 2000). Moreover, when fluorescently labelled casein was added as a macromolecular model compound to the coacervation process, a gradiental distribution of casein in the shell materials was observed. It was found that casein had the highest concentration at the oil-wall interface. In another study, CLSM was demonstrated to be effective in studying the distribution of polymers and cross-linking ions in alginate-poly-L-lysine (PLL)-alginate encapsulates made by fluorescent-labelled polymers (Strand et al. 2003).

Transmission Electron Microscopy

Due to the limitation of optical microscopy, transmission electron microscopy (TEM) that is capable of resolving structures with smaller dimensions than optical microscopy has often been used (Mathiowitz 1999). TEM focuses electrons emitted by a heated filament to provide images restricted only by wavelength of electrons, which are approximately 0.003 nm. TEM must be operated under high vacuum to prevent collisions of electrons with air molecules, which can cause losses in resolution. Electromagnets are also used to provide sufficient energy to penetrate samples. TEM has been used as reliable microscopy to quantify the morphology and shell thickness of encapsulates (Xu and Du 2003; Chiu et al. 2005). Figure 4.1 shows a TEM micrograph of an encapsulate with a core of chamomile oil. However, this technique is time consuming as sample preparation can be quite tedious.

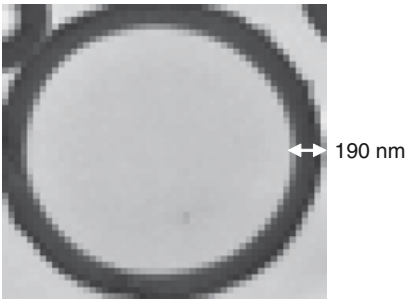

Fig. 4.1 TEM micrograph of a melamine formaldehyde micro-capsule encapsulating chamomile oil (Courtesy of Ms Yue Long, University of Birmingham, UK)

Scanning Electron Microscopy

Scanning electron microscopy (SEM) has a resolution of approximately 3 nm, which has the feature of simplicity in sample preparation and ease of operation. It has a great advantage because of its capability to analyse samples ranging in size from nano-metre to centimetre scale (Weiss et al. 1995; Shu et al. 2006; Yan-yu et al. 2006; Roueche et al. 2006). The spacious chamber and goniometer of a scanning electron microscope can accommodate relatively large samples as compared to a transmission electron microscope and provide nearly unlimited points of viewing with the assistance of translational, tilting, and rotary movements. Nonetheless, SEM does not distinguish colours as optical microscopy does and has lower resolution compared to TEM.

Environmental Scanning Electron Microscopy

Environmental Scanning Electron Microscopy (ESEM) offers several important advances in scanning electron microscopy. While a conventional scanning electron microscope requires a relatively high vacuum in the specimen chamber to prevent atmospheric interference with primary or secondary electrons, an environmental scanning electron microscope may be operated with a low vacuum (up to 10 Torr of vapour pressure, or one 76th of atmosphere pressure) in the specimen chamber and allows "wet mode" imaging, which is essential to investigate the surface tomography of wet encapsulates (Ren et al. 2007).

4.2.1.2 X-Ray Micro-computed Tomography

X-ray micro-computed tomography (CT) is an increasingly popular method to image complex three-dimensional structures with a spatial resolution in the micrometre range. The schematic diagram of an X-ray micro-CT system is shown in Fig. 4.2. The principle of this technique is by firstly acquiring X-ray images of an object placed between the X-ray source and the detector. Then the X-ray images are reconstructed and analysed using a commercially available software package. X-ray micro-CT offers the advantage of being a non-invasive and non-destructive testing method. Unlike some other testing methods, defects (including delamination, micro-cracking, fibre fracture, fibre pullout, matrix cracking, inclusions, voids, and impact damage) created during the preparation of the sample, which is required to adapt to a particular testing environment, can be avoided (Schilling et al. 2005). In addition, X-ray micro-CT allows unobstructed visual access to a sample's inner architecture in a completely non-destructive way and reconstructs interior structural details with a resolution on a scale of interest for such evaluation. It provides accurate details of variation of X-ray absorption within an object regardless of its structure properties and density gradients (Stock 1999). Previously X-ray micro-CT has been used successfully for quantitative measurements of localised density variations in cylindrical

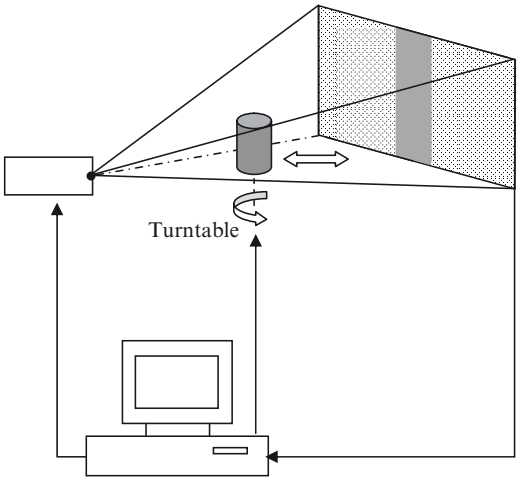

Fig. 4.2 Schematic diagram of the X-ray micro-computed tomography system

tablets. In all cases, an important heterogeneity in density was observed with higher densities concentrated in the peripheral region and lower densities in the middle (Busignies et al. 2006). This technique was also proven to be feasible to characterize the irregular interconnected pore structure of actual particle beds in order to study the fluid transport phenomena in a filter cake (Lin and Miller 2004). Recent work has shown that the internal structure of a calcium shellac bead can be characterized (see Fig. 4.3). However, the X-ray micro-CT cannot detect fine pores such as gel pores less than 0.01 μm (Rattanasak and Kendall 2005) and pores in granules less than 4 μm in diameter (Farber et al. 2003).

4.2.1.3 Laser Light Scattering

Although microscopy combined with image analysis can be used to measure the size of single encapsulates, it is a relatively slow technique particularly if a large number of encapsulates need to be measured. For spherical encapsulates, in wet or dry samples, with particles in the size range of 0.02–2,000 μm, measurement of their size distribution can be carried out using a laser light scattering technique, such as Malvern particle sizing, which can measure thousands of encapsulates within a couple of minutes. However, the refractive indexes of the shell material and the suspending medium are required. A similar technique to laser light scattering called single particle optical sensing (SPOS) has also been used to measure particle size distribution (O'Hagan et al. 2005). SPOS is based on measurement of the magnitude of pulse generated by single particles passing though a small photozone, illuminated by light from a laser diode or incandescent bulb, which can be correlated with the size of the particles. For non-spherical encapsulates or encapsulates which tend to form aggregates, microscopy combined with image analysis is

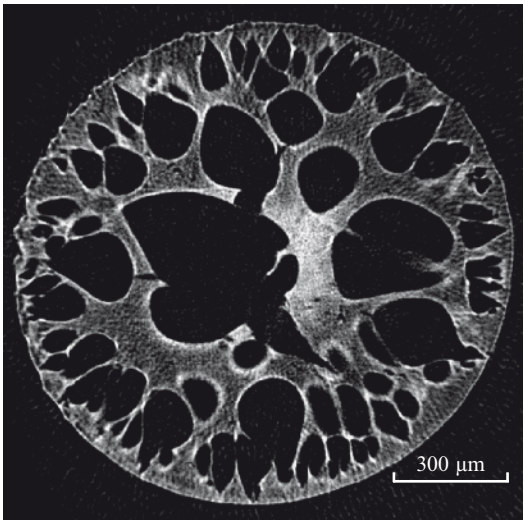

Fig. 4.3 Two-dimensional image of the central layer of a calcium shellac bead, which was reconstructed from pictures taken by X-ray micro-computed tomography (Law 2007)

preferred. Recently, a technique based on focused beam reflectance measurement (FBRM) has been used to provide in situ/on-line characterization of non-spherical particles by measuring chord lengths of particles, which are converted to particle size and shape of the particles by a mathematical model (Li et al. 2005). However, the data obtained by this technique require validation.

The electro kinetic potential in a suspension with encapsulates may be characterised by their zeta potential. It is a measure of the magnitude of the repulsion or attraction forces between encapsulates, which has a unit of mV. The value may be related to the storage stability of the encapsulates in suspension. In general, a particulate system with zeta potential smaller than −35 mV or greater than 35 mV tends to be stable (Legrand et al. 1999). Zeta potential can be measured by applying an electric field across the suspension. Encapsulates within the suspension with a zeta potential will migrate toward the electrode of opposite charge with a velocity proportional to the magnitude of the zeta potential. This velocity can be measured using laser Doppler anemometry. The frequency shift or phase shift of an incident laser beam caused by these moving encapsulates is measured as the particle mobility, which can be converted to the zeta potential by inputting the dispersant viscosity. Typical instruments for such measurement include Malvern Zetasizer Nano-Z (Malvern Instruments, UK).

It has been reported that the zeta-potential of polyamide encapsulates in suspension depends on the pH, concentration of electrolytes and surfactants in the suspension. Increasing the ionic strength led to a decrease in the zeta potential (Yan et al. 1992). Labhasetwar and Dorle (1991) measured the zeta potential of gelatin,

methylcellulose and agar encapsulates at regular intervals during ageing at 45°C. It was found that there was an initial sharp rise in Zeta potential followed by a progressive decrease. This demonstrates that zeta potential is a useful parameter to investigate the changes occurring in the encapsulating material of encapsulates during ageing. Some encapsulates can be made using a layer-by-layer deposition, e.g. poly-L-lysine (P-Lys) and poly-L-aspartic acid (P-Asp) onto a negatively charged liposome. The zeta potential of such encapsulates changed between positive and negative at each layer deposition (Fujimoto et al. 2007).

4.2.2 Mechanical Characterization

Different techniques have been developed to characterize the mechanical properties of encapsulates, which can be classified into indirect and direct methods. A cone and plate shearing apparatus was established to measure the mechanical strength of encapsulates by determining their resistance to fluid shear force (Peirone et al. 1998). Alternatively, encapsulate strength was evaluated by determining the percentage of intact encapsulates remaining after being agitated with glass beads for a period of time (Leblond et al. 1996), or exposing them to bubble disengagement in a bubble column (Lu et al. 1992). The results from these indirect methods are difficult to interpret since the damage to the encapsulates depends not only on their mechanical strength, but also on the hydrodynamics of the process equipment, which is poorly understood. For semi-permeable encapsulates, an osmotic pressure test was implemented providing a rapid means of assessing their mechanical stability (Van Raamsdonk and Chang 2001).

Direct methods include compression of a layer of encapsulates between two glass plates. Their mechanical strength was determined based on the number of encapsulates broken under a given applied weight on the top plate, but it was observed that the weight concentrated onto the largest encapsulates first caused them to break, followed by the smaller ones (Ohtsubo et al. 1991). Although this method is practically useful, it conceals (any) difference in mechanical strength between encapsulates within a sample. Despite being more time consuming, results attained from the assessment of single encapsulates is more accurate and reliable as compared with a sample of encapsulates because the inhomogeneity of encapsulates in the sample due to their variations in size and structure can be identified (Schuldt and Hunkeler 2000). Direct methods on single encapsulates include the use of a micropipette aspiration technique or an atomic force microscope probe to measure the elastic properties of single encapsulates. Unfortunately, the former technique cannot be used to determine the force required to rupture the encapsulates (Grigorescu et al. 2002), whilst the latter relies on compression of single encapsulates between a rigid spherical bead and a flat surface (Lulevich et al. 2003), which is difficult to implement. A uniaxial compression of single encapsulates was attempted by means of a texture analyser consisting of a penetrometer with a stress gauge (Edwards-Levy and Levy 1999). It provided a measure of a particle's resistance

to compressive force. However, assessment of single encapsulates was often prevented when their size went down to μm range (Martinsen et al. 1989). The limitation may be overcome by using a novel micro-manipulation technique that offers the capability to obtain the force vs. deformation data for compressing single encapsulates to rupture. The schematic diagram of a micro-manipulation rig is given in Fig. 4.4. The principle of this technique is to compress single encapsulates (dry or wet) between a probe connected with a force transducer and surface of a glass slide or glass chamber. The force transducer is connected with a fine micro-manipulator and its moving speed and distance can be controlled accurately. When single micro-encapsulates are compressed, the force imposed on them and their displacement are measured simultaneously. Moreover, the three-dimensional deformation of the encapsulates are also measured by two video cameras (for side view and bottom view respectively) connected to a video recorder or a computer with two image capture cards. This technique was initially used to measure the bursting strength of single animal cells, but later explored to mechanically characterize various biological and non-biological particles, including micro-spheres, encapsulates, etc. (Zhang et al. 1991; Zhang et al. 1992; Zhang et al. 1999; Stenekes et al. 2000; Sun and Zhang 2001; Zhao and Zhang 2004; Chung et al. 2005).

The micro-manipulation technique has been used to measure the mechanical strength of encapsulates of different size, shell thickness and shell composition (Zhang et al. 1999; Sun and Zhang 2001, 2002; Zhao and Zhang 2004). For example, the mechanical properties of single melamine formaldehyde (MF) encapsulates with diameters of 1–12 μm were determined, including their viscoelastic and elastic-plastic properties (Sun and Zhang 2001). It was found that the encapsulates were mainly elastic up to a deformation of 19 ± 1%. Beyond this point, the encapsulates underwent plastic deformation and were ruptured at a deformation of 70 ± 1%. However, the corresponding deformations at the yield point and at the rupture of

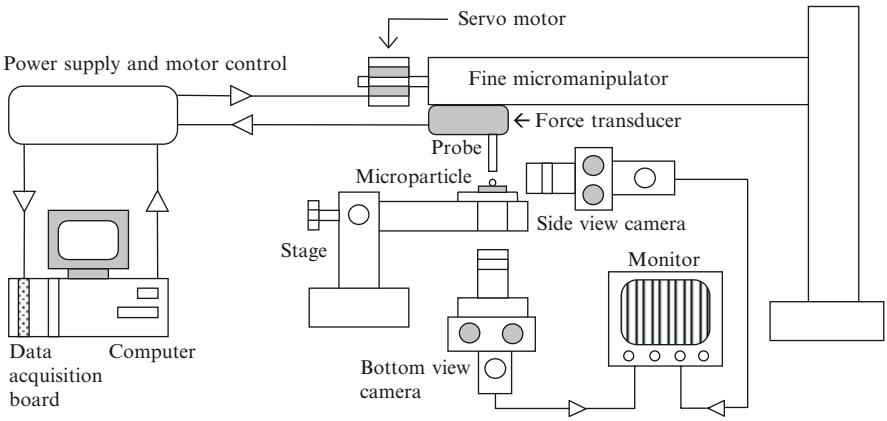

Fig. 4.4 Schematic diagram of the micro-manipulation rig. Permitted by Taylor & Francis

urea-formaldehyde encapsulates were 17 ± 1% and 35 ± 1% respectively, which implies that urea-formaldehyde encapsulates were more brittle than melamine formaldehyde (Sun and Zhang 2002). Besides the shell composition, the rupture strength of these encapsulates depended on their size and shell thickness. From the micromanipulation measurements the rupture force of different encapsulates can be compared by extracting information from a force-displacement curve up to the rupture. The curve can also be fitted with theoretical equations derived from a theoretical model, e.g. Lardner and Pujara's model (Lardner and Pujara 1980; Liu et al. 1996). This was used to determine the intrinsic mechanical property parameters, for example Young's modulus, and for further mathematical modeling to determine viscous-elastic and plastic parameters when appropriate. Such information is essential for quantifying the mechanical properties of encapsulates for a given sample and comparing the mechanical properties between different formulations.

Some encapsulates, e.g. calcium alginate beads, have certain permeabilities. When they are compressed, there can be a loss of liquid from the encapsulates and consequently their rupture force depends on the compression speed (Zhao and Zhang 2004; Wang et al. 2005). In order to minimise the speed-dependent behavior such encapsulates can be compressed at a high speed, e.g. 1,000 μm/s, which can be achieved using a newly developed micro-manipulation rig (Wang et al. 2005). This new high speed micro-compression tester, with two complementary high-speed videos, is a powerful tool for investigating the mechanical properties of hydrated encapsulates at the micro-scale.

The mechanical properties of single hydrated dextran encapsulates (<10 μm in diameter) with a model protein drug embedded were also measured by the micromanipulation technique, and the information obtained (such as the Young's modulus) was used to derive their average pore size and further to predict the protein release rate (Stenekes et al. 2000).

For encapsulates at the submicron scale, the above described micro-manipulation technique based on using conventional microscopy is not adequate to image single encapsulates clearly. Very recently, a novel ESEM-based nano-manipulation technique has been developed to characterize encapsulates at nano-scale. ESEM is primarily used to visualise materials on nano-scales under wet mode (Liu et al. 2005). To enable the mechanical properties of single encapsulates on such small scales to be measured, a nano-manipulation device with a force transducer was placed in the chamber of an environmental scanning electron microscope, and was used to compress single encapsulates and then measure the force imposed on them simultaneously. The nano-manipulation technique has been applied to investigate the mechanical properties of melamine formaldehyde (MF) encapsulates including their fracture mode (see Fig. 4.5) (Ren et al. 2007).

Understanding the mechanical strength of encapsulates is essential to a wide range of applications in controlled release of active ingredients including food encapsulates. Although not much work has been done on single food encapsulates, it is believed that the micro-/nano-manipulation technique described is a very powerful and unique tool to determine the mechanical properties of encapsulates made of different materials and structures.

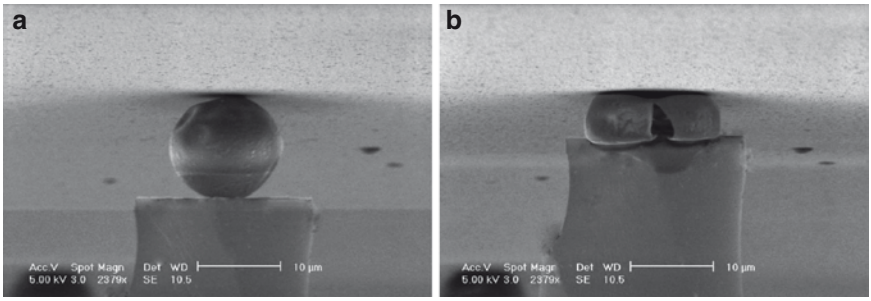

Fig. 4.5 A single melamine formaldehyde micro-capsule held between a force probe and a slide in the chamber of an environmental scanning electron microscope: (**a**) before compression; (**b**) after rupture. Permitted by Maney Publishing

4.2.3 Determination of Glass Transition and Degree of Crystallinity

The structure of encapsulates defines how the molecules in encapsulates are organised. Two parameters are often used to characterise the fine structure of encapsulates: glass transition temperature of encapsulates and crystallinity of encapsulate shell materials. These parameters may be used in designing encapsulates with desirable mass transfer properties (Le Meste et al. 2002).

4.2.3.1 Glass Transition Temperature

Glass transition temperature (T_g) is a property parameter of an amorphous material above which it behaves like a liquid (rubbery state) and many of the physical properties of the material change dramatically, including increase in heat capacity. Therefore, T_g can be determined by the measurement of a sudden increase in heat capacity with temperature, often using differential scanning calorimetry (DSC) (Bhandari and Howes 1999). DSC is a thermo analytical technique for measuring the energy required to maintain zero temperature difference between a sample and a reference (Hu et al. 2007). A similar technique to DSC is thermo gravimetric analysis (TGA), which is based on measuring weight changes associated with transformations of a material on heating (Foster and Clifford 1966), and has been used to identify the thermal decompositions of a copolymer (Shukla and Srivastava 2004).

Below the T_g the diffusion through carrier material is limited in a manner similar to those of a crystalline phase (glassy state). Above the T_g the carrier material is in rubbery state and the diffusion of molecules is relatively fast. This phenomenon can be used to design encapsulates that are storage stable below the T_g, which triggers release above a certain temperature.

Understanding the glass transition temperature may also be used to control the pore size of encapsulate shells. For example, encapsulates can be formed by close

packing of a layer of polymer particles, e.g. poly(methyl methacrylate) (PMMA) at the interface of the oil/water (O/W) droplets and such systems have been called "colloidosomes" (Dinsmore et al. 2002). The adsorbed polymer particles were then swollen with further monomer and an initiator to effect further polymerisation in the particle shell layer, causing the particles therein to first bridge and then to grow into a more continuous film. This process was aided by heating the system at 105°C for 5 min, which is above the glass transition temperature ($T_g = 100$°C) of the polymer. It was found that after heating; the particles coalesced slightly, creating approximately 150-nm-diameter bridges between them. The resultant colloidosome therefore contained a precise array of uniform holes in an elastic shell. Increasing the sintering time led to smaller pores: after 20 min, the particles coalesced completely and the holes were fully closed.

Besides, measurement of the glass transition temperature can help to understand interactions between the molecules of core and shell materials. Sasaki et al. (2006) used DSC to measure T_g of encapsulates consisting of calcium carbonate whisker as a core and crosslinked polystyrene as a shell. The crosslinked shell was found to show higher glass transition temperatures (T_g) than the corresponding bulk values. It was also revealed that a thicker shell exhibited a lower T_g than a thinner shell, and that encapsulates without the core (hollow encapsulates) exhibited lower T_g than the corresponding core/shell encapsulates.

4.2.3.2 Degree of Crystallinity

The degree of crystallinity of the encapsulate shell materials can be characterised by DSC, X-ray diffraction (XRD) or nuclear magnetic resonance (NMR).

In addition to glass transition temperature, DSC can also be used to characterise crystalline melt temperatures. From knowledge of both the glass transition temperature and crystalline melt properties, information regarding the degree of crystallinity can be obtained. XRD relies on measurement of a diffraction pattern generated when an encapsulate specimen is irradiated with a parallel beam of monochromatic X-rays and the atomic lattice of the specimen acts as a three-dimensional diffraction grating causing the X-ray beam to be diffracted to specific angles. The angles and intensities of the diffracted beam can be used to infer the degree of crystallinity. NMR is a technique based on monitoring how spinning nuclei with magnetic dipoles interact with an applied magnetic field and absorb radiation (Seamus 2003; Jonathan 2003). It was found that the spectrum of NMR can be separated into two components: a broad component associated with the rigid crystalline region and a narrow component associated with mobile non-crystalline regions (Montes de Oca et al. 2004). NMR is designed for structural determination and analytical applications.

Ricciardi et al. (2004) used DSC, XRD and NMR to measure the degree of crystallinity of poly(vinyl alcohol) (PVA) hydrogels, and demonstrated that these three methods had different accuracies, which depended on the complexity of their structure.

The degree of crystallinity of polyamide capsules was estimated by XRD (Yoshioka et al. 2007), which were prepared from reacting diamines and diacid chlorides in an acetone or dioxane solution that included water, using the precipitation polymerization method employing ultrasonic irradiation. They found that the degree of crystallinity greatly depended on the combination of the diamine compound, diacid chloride compound, and reaction solvent.

The permeabilities of the polyurea micro-capsules for encapsulated cyclohexane were determined in conjunction with the degree of crystallinity of the polymer forming the membranes by XRD (Yadav et al. 1997). For cyclohexane diffusion through the water-swollen polyurea membranes used in their work, the permeability ranged from 6.5×10^{-9} to 3.75×10^{-8} m/s. It was shown that the product of the permeability and membrane thickness varied over an order of magnitude when the degree of crystallinity was changed from 21% to 33%.

In another study, nano-capsules based on polyureas and polyamides were prepared based on polycondensation reaction of two complementary monomers and spontaneous formation of oil in water emulsion. It has been found that the permeability of the polymeric wall of polyureas and polyamides was related to its crystallinity (Montasser et al. 2007).

4.2.4 Flowability of Dry Encapsulates

Dry encapsulates are like powders and their flowability is important in handling and processing operations, such as flow from hoppers and silos, transportation, mixing, compression, processing and packaging (Fitzpatrick et al. 2004a, b). The standard techniques to characterize the flowability of powders can also be applied to encapsulates although attention should be paid to handling encapsulates in order to minimise their mechanical damage.

Regarding the methods to characterize flowability of powders, Schulze (1996a, b) compared 16 flowability test methods of powders and concluded that the Jenike shear test was the most accurate method. Shear cell techniques for measuring powder flow properties were pioneered by Jenike (1964). In short, the horizontal shear forces needed to make a powder flow are measured as a function of different vertical pressures. A comprehensive explanation of the fundamental of shear cell techniques and schematic diagram can be found in Fitzpatrick et al. (2004a) and Carson and Wilms (2006). In conjunction with the data obtained from a shear cell technique, Jenike developed a theoretical background for the flow of solids from silos, a tester to determine the relevant flow properties, and a design procedure consistent with theory, flow properties, and industrial practice. Jenike test has been used to determine the influence of relative humidity and temperature on the flowability of different food powders (Teunou and Fitzpatrick 1999). However, the main disadvantage of Jenike test is that it is difficult to conduct (Zou and Brusewitz 2002). So far, there has not been much work in the public domain on the flowability of dry encapsulates.

4.3 Mass Transfer

In this section, the mechanisms of mass transfer that underpin the application of encapsulation are discussed. The emphasis has been placed on the mathematical modelling and experimental characterization of the fundamental factors that affect mass transfer, including solute partition and equilibrium, interfacial mass transfer and rate limiting steps.

4.3.1 Mass Transfer Mechanisms

Release of active ingredients from encapsulates can be induced or triggered by various methods including diffusion, mechanical rupture, melting, dissolution, hydration, enzyme attack, chemical reaction, hydrolysis, disintegration and so forth. In the food industry, the most commonly used method to trigger controlled release is by hydration. For example, the active is released from dry products when water is added. The release of the active from encapsulates depends on several mutually interacting processes such as diffusion of the flavor compound through the matrix, type and geometry of the particles, transfer from the matrix to the environment, and degradation/dissolution of the matrix material (Pothakamury and Barbosa-Canovas 1995). The dynamics of hydration and enzymatic reactions of the matrix with saliva also have important effects.

The physical process of controlled release of active ingredients from encapsulates can be described by diffusion and/or convection or a combination of both. The driving force of diffusion is the gradient in the chemical potential of the active ingredients between encapsulates and the surrounding environment. Convective mass transfer can be triggered by hydration, phase change, pH change, reaction and mechanical fracture of encapsulates. A good example of convective mass transfer is the mechanical rupture of micro-encapsulated flavor by chewing.

Other methods used to trigger controlled release include changes in pH and temperature. Karel and Langer (1988) reported a study on controlled release of enzymes from liposomes through the change in pH. Release of actives can also be triggered by the melting of wall material composed of lipids or waxes. Components such as salts, leavening agents, flavorings and nutrients are released when the shell is destroyed by melting. Encapsulates made of hardened fats are insoluble in water and the content can be released when they are subjected to shear or increased temperature which melts the fat. This type of encapsulates is widely used in soup mixes, bakery products or high-fat products (Dziezak 1988). The release of active ingredients depends strongly on the heat transfer that governs the melting process. Yeo et al. (2005) reported a study on flavor encapsulation in complex coacervate encapsulates using gelatin and gum arabic. Solubility of their encapsulate shell was temperature dependant.

In drug delivery, osmotic trigger has also been used. Molecules such as glucose, hydroxyethylcellulose, glycerol, poly (ethylene glycol)s, and dextrans of different

molecular weights are extensively employed as osmotic agents (Santus and Baker 1995; Verma et al. 2002). The osmotic agents form the expandable core contained within a semi-permeable compartment. Pharmaceutical agent held within is released during the expansion and disintegration of the core material. Hydrogels have also attracted wide research interest as controlled release devices due to their tunable chemical and three-dimensional physical structure, high water content, good mechanical properties, and biocompatibility (Langer and Peppas 2003). Bioresponsive, "intelligent" or "smart" hydrogels can regulate drug release through responding to environmental stimuli by swelling and deswelling. Various bioresponsive and thermoresposive hydrogels have been developed for drug delivery (Zhang and Chu 2002; Huang et al. 2004).

For encapsulation in food industry, much of the challenge is balancing the need in protecting active molecules during processing and storage (from oxidation, leaking, and loss by evaporation) and controlling the rate of release to achieve optimal effect. Drying of the encapsulates/granules to a glassy state is a well-established technology and various drying processes have been developed including spray drying, fluidized bed drying, freeze drying, extrusion and microwave drying. In a dry glassy state, diffusion of active molecules is prohibited. The release of the active is triggered when dry encapsulates are hydrated. Diffusion of active molecules in hydrated matrix and/or dissolved solution becomes orders of magnitudes faster.

4.3.2 Mass Transfer Properties

A major challenge in controlled release is to understand the complex interactions of various dynamic processes accompanying the mass transfer. In particular, the dynamics of heat transfer, phase change, reaction, hydrolysis and hydration all have profound impact on the mass transfer properties of encapsulates. Understanding such complex interplay that governs the active release from encapsulates is critical.

Many researchers have sought a better understanding of the effects that govern the release of active ingredients from complex matrices of encapsulates as this represents an important target in many fields, including the food industry (Guichard 2000). An overview of physical chemistry relevant to flavor release has been presented previously (Taylor 1998). De Roos (2000) showed that two factors control the rate of flavor release from products, the comparative volatility of the aroma compounds in the food matrix and air phase under equilibrium conditions (thermodynamic factor) and the resistance to mass transport from product to air (kinetic factor).

Most encapsulates have complex heterogeneous structures. A wide range of materials can be selected for encapsulation. Micro-encapsulates can be made of sugars, gums, proteins, natural and modified polysaccharides, lipids and synthetic polymers (see Chap. 3 of this book). For food applications, the selection is somewhat limited because food safety is an additional consideration.

Mass transfer in heterogeneous encapsulates is exceedingly complex. A number of studies have been reported on the diffusion in complex networks of synthetic

and/or biological gels (e.g. Kosto and Deen 2005; Pluen et al. 1999; Amsden 1998; Fatin-Rouge et al. 2003; Johnson et al. 1996; Phillips et al. 1989; Odijk 2000; Phillips 2000). Theoretical models proposed include hindered diffusion by hydrodynamic interaction, trapped diffusion by excluded structure volume and depletion theory. Diffusion and partition of solutes in lipid has received considerable attention.

Mass transfer in heterogeneous encapsulates depends strongly on the environmental condition under consideration. A good knowledge of the physico-chemical interactions occurring between compounds and the main constituents of foods such as lipids, polysaccharides, and proteins, is required for food active control. Mass transfer in complex encapsulates depends not only on the diffusion property but also on the thermodynamic properties such as gas-liquid equilibrium (for volatiles) and liquid-solid equilibrium.

4.3.2.1 Gas-Liquid Equilibrium for Release of Volatiles

Gas-liquid equilibrium is an important property of mass transfer of volatiles from encapsulates with a liquid core and/or liquid foods. When a volatile substance is added to a gas-liquid system, the substance will distribute itself in the liquid and gas phases. At equilibrium, the partial pressure of a volatile compound in the gas phase is related to its concentration in the liquid solution. In dilute solution, this relationship is described by Henry's law

$$p_{\mathrm{i}} = Hx_{\mathrm{i}} \tag{4.2}$$

where p_{i} is the partial pressure of a volatile compound in headspace, x_{i} is the mole concentration in the liquid solution, and H is Henry's constant.

For ideal gas, the partial pressure of volatile can be related to its mole fraction in the headspace and the atmosphere pressure by the relationship $y_i = p_i/P_0$. The other form of Henry's law is written as

$$y_{\mathrm{i}} = \frac{H}{P_0} x_{\mathrm{i}} = mx_{\mathrm{i}} \tag{4.3}$$

Net flux of mass transfer between gas and liquid takes place if the gas-liquid equilibrium is violated.

4.3.2.2 Gas-Solid Equilibrium for Release of Volatiles and Water Sorption Isotherm

Another important mass transfer property of encapsulates might be gas-solid equilibrium. The relationship is characterised by the sorption isotherm. The sorption of oxygen on encapsulates is related to the oxidation of lipids and other labile materials. The sorption of water vapour by encapsulates has received much attention because of its important effect on the storage and controlled release properties.

Water sorption isotherm is described by water activity (a_w), which is defined as the ratio of the partial pressure of water vapour at equilibrium, p_w, to the corresponding saturated vapour pressure, p_{sat}

$$a_w = \frac{p_w}{p_{sat}} \tag{4.4}$$

In other words, the water activity of a solid material is related to the relative humidity.

Water sorption isotherm of a given encapsulate system can be determined experimentally. Several empirical equations have been proposed. The Langmuir isotherm relates the water activity to adsorbed water content (θ_w) by

$$a_w\left(\frac{1}{\theta_w}-\frac{1}{\theta_0}\right)=\frac{1}{\beta\theta_0} \tag{4.5}$$

where θ_0 is the water content corresponding to the monolayer adsorption and β is a constant.

The other commonly used water sorption isotherm is the BET equation

$$\frac{a_w}{(1-a_w)\theta_w}=\frac{1+(\beta-1)a_w}{\beta\theta_0} \tag{4.6}$$

Water sorption isotherm has a number of effects on the mass transfer of active ingredient in encapsulates. Firstly, for many applications, hydration triggers the release of active ingredients. Secondly, water sorption isotherm has strong interaction with solute diffusivity of matrix materials. Thirdly, water vapor adsorption by encapsulates changes the quality of encapsulates during storage and transportation.

4.3.2.3 Solute Partition and Adsorption

Emulsions and dispersions are common structures of fabricated foods. When an active molecule such as flavor is added to a system of two immiscible phases, the solute may distribute itself in the two phases to reach equilibrium. The ratio of the concentrations of a solute in the two phases is called the partition coefficient. The partition coefficient of a solute in two immiscible fluids is relatively insensitive to temperature and concentration. The relationship is expressed by the following equation

$$C_y = KC_x \tag{4.7}$$

where K is the partition coefficients, and C_x, C_y are the concentrations of a solute in phase X and Y respectively.

Liquid-liquid equilibrium can also be extended to describe the partition of a solute binding and absorption to dispersed particles of complex fluids. The binding

of volatile compounds to starch has been classified into two types. On the one hand, the flavor compound surrounded by the amylose helix through hydrophobic bonding is known as an inclusion complex. On the other hand, polar interactions have been determined which involve hydrogen bonds between the hydroxyl groups of starch and aroma compounds.

Of the many immiscible liquid-liquid systems, octanol-water equilibrium is widely studied and has generated great interest. Octanol-water partition coefficient is noted as P_{ow} or K_{ow}. Experimental data of octanol-water partition coefficients are available for a large number of chemicals. Methods have also been proposed for calculating octanol-water partition coefficients based on the molecular structures of solute. The fragment or group contribution method and atomistic method are the most commonly applied methods. The reader is referred to the monograph of Sangster (1997) for more details on the fundamental physical chemistry of octanol-water partition, including the measurement and prediction methods.

4.3.2.4 Solute Diffusion in Complex Media

The theory of Fick's diffusion applies to homogeneous media. The use of Fick's diffusion equation to describe the mass transfer of encapsulates is an oversimplified view. For emulsions and dispersions, where the size of the dispersed particles is sufficiently small compared to that of the encapsulates, it is possible to use the effective diffusion coefficient which is related to the diffusion and partition properties of the continuous and dispersed phases as follows (Lian 2000)

$$D_e = D_c \frac{D_c(1-\varphi)\xi + P_{dc}D_d(1+\xi\varphi)}{D_c(\xi+\varphi) + P_{dc}D_d(1-\varphi)} \tag{4.8}$$

where φ is the volume fraction of the dispersed phase, P_{dc} the partition coefficient of solute between dispersed phase and continuous phase, D_c and D_d are the diffusion coefficients of the solute in the continuous phase and dispersed phase respectively.

Thus, even for relatively simple structures of dispersions and emulsions, the effective diffusion property depends not only on the diffusion coefficients of the two phases, but also on the partition coefficient. The above effective diffusion coefficient was used to predict aroma release from oil-containing gel particles dispersed in aqueous solution and there was a good agreement with the experimental data (Lian et al. 2004).

Solute diffusion in complex fluids is affected by both temperature and molecular size. The following Einstein-Stokes equation can be used to estimate the diffusion coefficient of the active (D) in carrier material:

$$D = \frac{KT}{6\pi\eta r} \tag{4.9}$$

where K is the Boltzman constant, T is the temperature (K), η is the viscosity (Pa s), and r is the hydrodynamic radius of the active. This equation shows that the diffusion and thus the active release out of encapsulates increases with increasing temperature, decreasing viscosity of the carrier material and decreasing molecular size of the entrapped active.

Solute diffusion in lipids can also be estimated using the following equation (Mitragotri 2002)

$$D_{\text{lip}} \approx D_0 \exp\left(-0.4r^2\right) \tag{4.10}$$

where D_0 is the diffusion coefficient in isotropic model hydro-carbon.

Diffusion of solute in complex networks of synthetic and/or biological gels has received significant attention (e.g. Kosto and Deen 2005; Pluen et al. 1999; Amsden 1998; Fatin-Rouge et al. 2003). Theoretical models proposed include hindered diffusion by hydrodynamic interaction, trapped diffusion by excluded structure volume and depletion theory (Amsden 1998).

4.3.3 Characterizing Mass Transfer Properties

Many of the physical-mechanical-structural properties of importance to the mass transfer of encapsulates have been discussed in the forgoing sections, for example, various microscopic methods for microstructure, DCS method for phase change and NMR for degree of crystallinity. Methods for characterizing the equilibrium properties (liquid-gas, solid-gas, and liquid-liquid) can be also found elsewhere (Rao and Rizvi 1994). Here, only methods for characterizing the dynamic mass transfer process of encapsulates are discussed.

4.3.3.1 Diffusion Cell

Diffusion cell can be used for measuring the diffusion properties of composite wall materials of encapsulates. The system is made of a membrane of the tested composite material separating two liquid-filled, well-stirred compartments. One compartment contains solute of a known concentration, whilst the other, known as the recipient side, is initially free of the solute. Measuring the concentration change with time allows the effective diffusion coefficient, D_e, to be obtained. The review by Westrin et al. (1994), concludes that the diffusion cell is a good method. However, the method is limited to encapsulate materials that can form thin membranes.

4.3.3.2 Release from Encapsulate Dispersion

The widely used method is to measure the release of active ingredients from encapsulates dispersed in a liquid media. Gentle agitation is applied to ensure good mixing and suspension of the dispersed encapsulates. The increase in solute concentration in the

liquid phase is measured to determine the release kinetics and effective diffusion coefficient, D_e. Measurement can be automated and continuous, if an online analysis method for the active ingredient is available. The method has been generally regarded as an established method for measuring the release kinetics from particular systems, such as the flavor release from tea leaf particles (Lian and Astill 2002).

4.3.3.3 MS-Breath

MS-breath is a relative new method for in-mouth flavor release measurement. The method involves the use of atmospheric pressure chemical ionisation or proton transfer-reaction mass spectroscopy (APCI-MS or PTR-MS) to measure the real time release of volatile compounds from the mouth and into the nasal headspace during eating. Exhaled air from the nose is gently sucked into the mass spectrometer where the concentrations of the volatile compounds are continuously detected as protonated ions. The main advantage of the MS-breath method is that it obtains real time release profile that can be directly correlated to sensory properties. However, the release of the volatile from encapsulates to the nasal headspace has several rate-limiting steps and a complicated mathematical model is required to obtain the mass transfer properties of encapsulates (Lian et al. 2004).

4.3.4 Modeling Release Kinetics

To characterize mass transfer properties of encapsulates, reliable mathematical models are required to predict the release kinetics and fit with experimental data. Modeling release kinetics is also important for designing encapsulate systems (material, structure, size and loading) to achieve the desired release rate. When a simple diffusion model is used to describe the release kinetics of solutes from encapsulates, mathematical equations can be derived for various shaped encapsulates. For a homogeneous spherical encapsulate under infinite sink condition, the amount of released material is related to the size by the following Crank equation

$$\frac{M_t}{M_0} = 1 - \sum_{n=0}^{\infty} \frac{6}{\pi^2 n^2} \exp\left(-\frac{D_e \pi^2}{R^2} n^2 t \right) \tag{4.11}$$

where M_t is the amount of material released from the encapsulate, M_0 is the initial loading, D_e is the effective diffusion coefficient of solute through the encapsulate matrix and R is the radius of the encapsulate.

Corresponding to the early stage of release, the equation can be approximated by

$$\frac{M_t}{M_0} = 6\left(\sqrt{\frac{D_e t}{\pi R^2}} - 3\frac{D_e t}{R^2} \right) \tag{4.12}$$

This forms the so-called penetration theory for modeling flavor release with repetitive surface renewal (Overbosch et al. 1991).

At longer time, (4.11) can be approximated by the following equation

$$\frac{M_t}{M_0} = 1 - \exp\left(-1.2\pi^2 \frac{D_e}{R^2} t\right) \tag{4.13}$$

This is the first-order release kinetics which has been widely used to describe solute release from dispersions of encapsulates. The half-time at which 50% of the contents of the encapsulates is released can be calculated from (4.13) as follows:

$$\frac{M_t}{M_0} = 1 - \exp\left(-1.2\pi^2 \frac{D_e}{R^2} t_{1/2}\right) = 0.5 \tag{4.14}$$

which results in

$$t_{1/2} = \frac{\ln(0.5) R^2}{1.2\pi^2 D} \tag{4.15}$$

Equation (4.13) might also be described as:

$$\frac{M_t}{M_0} = 1 - \exp\left[-kt\right] \tag{4.16}$$

The term first-order equation has historically been derived from the equation:

$$\frac{\partial(M_0 - M_t)}{\partial t} = k(M_0 - M_t)^n \tag{4.17}$$

where n is the reaction order. Solving this latter equation for $n = 1$ gives the first-order release equation. For zero-order release, one assumes that the release is not dependent on its concentration and therefore $n = 0$:

$$\frac{\partial(M_0 - M_t)}{\partial t} = k \tag{4.18}$$

which can also be integrated to obtain the following equation

$$\frac{M_t}{M_0} = kt \tag{4.19}$$

In the latter equation, $t < 1/k$. Please note zero-order kinetic provides constant release of actives with time (see Fig. 4.6). When the active ingredient loaded to an encapsulate system is over saturated, the release rate of encapsulated solute to an infinite sink environment becomes constant.

The temperature dependence of k might be described by the Arrhenius equation:

$$k = A\mathrm{e}^{-E_a/R_g T} \tag{4.20}$$

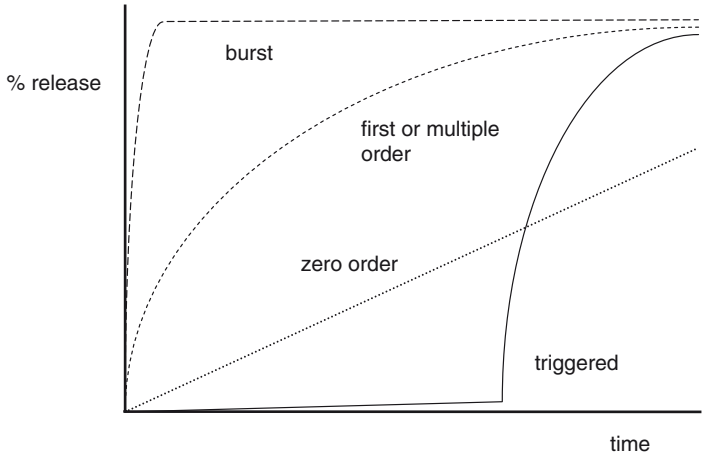

Fig. 4.6 Release profiles from encapsulates. Burst release is typical for soluble or broken ones. Release might also be triggered after a certain period of time by, e.g. pH change or addition of enzymes. Zero-order release is obtained with over saturated amounts of active in the core or with micro-capsules where the thin shell is the rate limiting step. First- or multiple-order release is common for matrix type of encapsulates and release due to other interactions. See also text

where A is the frequency factor, E_a is the activation energy, R_g is the gas constant.

Generally, encapsulates exhibit more complex release kinetics due to the interactions with other rate limiting steps such as hydration, structural breakdown and enzyme attack. Even for relatively simple systems such as in-mouth flavor release from oil-containing gel particles, there are two rate limiting steps, the release of aroma from gel particle to the saliva and the release of aroma from saliva to the retro nasal head space (Lian et al. 2004). The release kinetics exhibits two-components, corresponding to a fast component and a slow component. The gel effect of particle size interacts with the partition properties. Only for highly hydrophobic aroma molecules, the change of gel particle size has the expected effect.

4.4 Conclusions

The success of a formulation/encapsulation process depends on whether the formed encapsulates have desirable properties, including physical, mechanical, structural and mass transfer properties. In this chapter, the state-of-art methods which are currently used for characterization of these properties are reviewed. However, it seems that most of the published work on the characterization of the encapsulate properties focused on physical and mass transfer properties. Less attention has been paid to mechanical characterization, and a very limited amount of work has been done on

structural characterization, and the relationship between these properties. In the future, more efforts should be made toward understanding the mechanical and structural properties, and how they are related to physical and mass transfer properties.

References

Amsden B (1998) Solute diffusion in hydrogels. An examination of the retardation effect. Polym Gels Networks 31:13–43

Bhandari BR, Howes T (1999) Implication of glass transition for the drying and stability of dried foods. J Food Eng 40:71–79

Busignies V, Leclerc B, Porion P, Evesque P, Couarraze G, Tchoreloff P (2006) Quantitative measurements of localized density variations in cylindrical tablets using X-ray microtomography. Eur J Pharm Biopharm 64:38–50

Carson JW, Wilms H (2006) Development of an international standard for shear testing. Powder Technol 167:1–9

Chiu GNC, Abraham SA, Ickenstein LM, Ng R, Karlsson G, Edwards K, Wasan EK, Bally MB (2005) Encapsulation of doxorubicin into thermosensitive liposomes via complexation with the transition metal manganese. J Control Release 104:271–288

Chung JT, Vlugt-Wensink KDF, Hennink WE, Zhang Z (2005) Effect of polymerization conditions on the network properties of dex-HEMA microspheres and macro-hydrogels. Int J Pharm 288:51–61

De Roos KB (2000) Physicalchemical models of flavor release from foods. In: Roberts DD, Taylor AJ (eds) Flavor release, ACS Symposium Series 763. American Chemical Society, Washington, DC

Dinsmore AD, Hsu MF, Nikolaides MG, Marques M, Bausch AR, Weitz DA (2002) Colloidosomes: Selectively permeable capsules composed of colloidal particles. Science 298:1006–1009

Dziezak JD (1988) Microencapsulation and encapsulated ingredients. Food Technol 42:136–151

Edwards-Levy F, Levy M-C (1999) Serum albumin-alginate coated beads: mechanical properties and stability. Biomaterials 20:2069–2084

Farber L, Tardos G, Michaels JN (2003) Use of X-ray tomography to study the porosity and morphology of granules. Powder Technol 132:57–63

Fatin-Rouge N, Milon N, Buffle J, Goulet RR, Tessier A (2003) Diffusion and partitioning of solutes in agarose hydrogels: the relative influence of electrostatic and specific interactions. J Phys Chem B 107:12126–12137

Fitzpatrick JJ, Barringer SA, Iqbal T (2004a) Flow property measurement of food powders and sensitivity of Jenike's hopper design methodology to the measured values. J Food Eng 61:399–405

Fitzpatrick JJ, Iqbal T, Delaney C, Twomey T, Keogh MK (2004b) Effect of powder properties and storage conditions on the flowability of milk powders with different fat contents. J Food Eng 64:435–444

Foster DS, Clifford LH (1966) Encyclopedia of industrial chemical analysis. Interscience, New York

Fujimoto K, Toyoda T, Fukui Y (2007) Preparation of bionanocapsules by the layer-by-layer deposition of polypeptides onto a liposome. Macromolecules 40:5122–5128

Grigorescu G, Rosinski S, Lewinska D, Ritzén LG, Viernstein H, Teunou E, Poncelet D, Zhang Z, Fan X, Serp D, Marison I, Hunkeler D (2002) Characterization of microcapsules: recommended methods based on round-robin testing. J Microencapsul 19:641–659

Guichard E (2000) Interaction of food matrix with small ligands influencing flavour and texture – foreword. Food Chem 71:299–300

Hu Y, Zhang J, Sato H, Noda I, Ozaki Y (2007) Multiple melting behavior of poly(3-hydroxybutyrate-co-3-hydroxyhexanoate) investigated by differential scanning calorimetry and infrared spectroscopy. Polymer 48:4777–4785

Huang G, Gao J, Hu ZB, John JVS, Ponder BC, Moro D (2004) Controlled drug release from hydrogel nanoparticle networks. J Control Release 94:303–311

Jenike AW (1964) Storage and flow of solids. Bulletin 123, Engineering Experiment Station, University of Utah, USA
Johnson EM, Berk DA, Jain RK, Dean WM (1996) Hindered diffusion in argarose gels: test of effective medium model. Biophys J 70:1017–1026
Jonathan AI (2003) NMR spectroscopy in inorganic chemistry. Oxford University Press, New York
Karel M, Langer R (1988) Controlled release of food-additives. ACS Symp Ser Am Chem Soc 370:177–191
Kosto KB, Deen WM (2005) Hindered convection of macromolecules in hydrogels. Biophys J 88:277–286
Labhasetwar VD, Dorle AK (1991) A study on the zeta potential of microcapsules during aging. J Microencapsul 8:83–85
Lamprecht A, Schafer UF, Lehr CM (2000) Characterization of microcapsules by confocal laser scanning microscopy: structure, capsule wall composition and encapsulation rate. Eur J Pharm 49:1–9
Langer R, Peppas NA (2003) Advances in biomaterials, drug delivery, and bionanotechnology. AIChE J 49:2990–3006
Lardner TJ, Pujara P (1980) Compression of spherical cells. Mechanics Today 5:161–176
Law NGD (2007) Stabilisation and targeted delivery of enzyme nattokinase by encapsulation. Doctoral Dissertation, The University of Birmingham, UK
Le Meste M, Champion D, Roudaut G, Blond G, Simatos D (2002) Glass transition and food technology: a critical appraisal. J Food Sci 67:2444–2458
Leblond FA, Tessier J, Halle JP (1996) Quantitative method for the evaluation of biomicrocapsule resistance to mechanical stress. Biomaterials 17:2097–2102
Legrand P, Barratt G, Mosqueira V, Fessi H, Devissaguet JP (1999) Polymeric nanocapsules as drug delivery systems. A review. STP Pharma Sci 9:411–418
Li MZ, Wilkinson D, Patchigolla K (2005) Determination of non-spherical particle size distribution from chord length measurements. Part 2: Experimental validation. Chem Eng Sci 60:4992–5003
Lian G (2000) Modeling flavor release from oil-containing gel particles. In: Roberts DD, Taylor AJ (eds) Flavor release. ACS Symposium Series 763. American Chemical Society, Washington, DC, pp 201–211
Lian G, Astill C (2002) Computer simulation of the hydrodynamics of teabag infusion. Food Bioproducts Processing 80:155–162
Lian GP, Malone M, Homan JE, Norton IT (2004) A mathematical model of volatile release in mouth from the dispersion of gelled emulsion particles. J Control Release 98:139–155
Lin CL, Miller JD (2004) Pore structure analysis of particle beds for fluid transport simulation during filtration. Int J Mineral Process 73:281–294
Liu KK, Williams DR, Briscoe BJ (1996) Compressive deformation of a single microcapsule. Phys Rev E 54:6673–6680
Liu T, Donald AM, Zhang Z (2005) Novel manipulation in environmental SEM for measuring the mechanical properties of single nano-particles. Mater Sci Technol 21:289–294
Lu GZ, Thompson FG, Gray MR (1992) Physical modelling of animal cell damage by hydrodynamic forces in suspension cultures. Biotechnology and Bioengineering 40:1277–1281
Lulevich VV, Radtchenko IL, Sukhorukov GB, Vinogradova OI (2003) Deformation properties of nonadhesive polyelectrolyte. J Phys Chem B 107:2735–2740
Martinsen A, Skjakbraek G, Smidsrød O (1989) Alginate as immobilization material. 1. Correlation between chemical and physical properties of alginate gel beads. Biotechnol Bioeng 33:79–89
Mathiowitz E (1999) Encyclopedia of controlled drug delivery. Wiley, New York
Mitragotri S (2002) A theoretical analysis of permeation of small hydrophobic solutes across the stratum corneum based on scaled particle theory. J Pharm Sci 91:744–752
Montasser I, Briancon S, Fessi H (2007) The effect of monomers on the formulation of polymeric nanocapsules based on polyureas and polyamides. Int J Pharm 335:176–179
Montes de Oca H, Ward IM, Klein PG, Ries ME, Rose J, Farrar D (2004) Solid state nuclear magnetic resonance study of highly oriented poly(glycolic acid). Polymer 45:7261–7272

O'Hagan P, Hasapidis K, Coder A, Helsing H, Pokrajac G (2005) Particle size analysis of food powders. In: Onwulata C (ed) Encapsulated and powdered foods. CRC, Boca Raton, FL, pp 215–245
Odijk T (2000) Depletion theory of protein transport in semi-dilute polymer solutions. Biophys J 79:2314–2321
Ohtsubo T, Tsuda S, Tsuji K (1991) A study of the physical strength of fenitrothion microcapsules. Polymer 32:2395–2399
Overbosch P, Agterhof WGM, Haring PMG (1991) Flavour release in the mouth. Food Reviews International 7(2):137–184
Peirone MA, Delaney K, Kwiecin J, Fletch A, Chang PL (1998) Delivery of recombinant gene product to canines with nonautologous microencapsulated cells. Hum Gene Ther 9:195–206
Phillips RJ (2000) Hydrodynamic model for hindered diffusion of proteins and micelles in hydrogels. Biophys J 79:3350–3353
Phillips RJ, Dean WM, Brady JF (1989) Hindered transport in fibrous memberanes and gels. AIChE J 35:1761–1769
Pluen A, Netti PA, Jain RK, Berk DA (1999) Diffusion of macromolecules in agarose gels: Comparison of linear and globular configurations. Biophys J 77:542–552
Pothakamury UR, Barbosa-Canovas GV (1995) Fundamental aspects of controlled release in foods. Trends Food Sci Technol 6:397–406
Rao M, Rizvi SSH (1994) Engineering properties of foods. Marcel Dekker, New York
Rattanasak U, Kendall K (2005) Pore structure of cement/pozzolan composites by X-ray microtomography. Cement Concrete Res 35:637–640
Ren Y, Donald AM, Zhang Z (2007) Investigation of the radiation damage to microcapsules in an Environmental SEM. Mater Sci Technol 23:857–864
Ricciardi R, Auriemma F, Gaillet C, De Rosa C, Laupretre F (2004) Investigation of the crystallinity of freeze/thaw poly(vinyl alcohol) hydrogels by different techniques. Macromolecules 37:9510–9516
Roueche E, Serris E, Thomas G, Perier-Camby L (2006) Influence of temperature on the compaction of an organic powder and the mechanical strength of tablets. Powder Technol 162:138–144
Sangster J (1997) Octanol-water partition coefficients: fundamentals and physical chemistry. Wiley Series in Solution Chemistry, New York
Santus G, Baker RW (1995) Osmotic drug-delivery. A review of the patent literature. J Control Release 35:1–12
Sasaki T, Kawagoe S, Mitsuya H, Irie S, Sakurai K (2006) Glass transition of crosslinked polystyrene shells formed on the surface of calcium carbonate whisker. J Polym Sci B Polym Phys 44:2475–2485
Schilling PJ, Karedla BR, Tatiparthi AK, Verges MA, Herrington PD (2005) X-ray computed microtomography of internal damage in fiber reinforced polymer matrix composites. Compos Sci Technol 65:2071–2078
Schuldt U, Hunkeler D (2000) Characterization methods for microcapsules. Minerva Biotechnologica 12:249–264
Schulze D (1996a) Measuring powder flowability: a comparison of test methods. Part I. Powder Bulk Eng 10:17–28
Schulze D (1996b) Measuring powder flowability: a comparison of test methods. Part II. Powder Bulk Eng 10:45–61
Seamus PJH (2003) Analytical chemistry. Oxford University Press, New York
Shiu C, Zhang Z, Thomas CR (1999) A novel technique for the study of bacterial cell mechanical properties. Biotechnol Tech 13:707–713
Shu B, Yu W, Zhao Y, Liu X (2006) Study on microencapsulation of lycopene by spray-drying. J Food Eng 76:664–669
Shukla A, Srivastava AK (2004) Synthesis and characterization of functional copolymer of linalool and vinyl acetate: a kinetic study. J Appl Polym Sci 92:1134–1143
Stenekes RJH, De Smedt SC, Demeester J, Sun GZ, Zhang ZB, Hennink WE (2000) Pore sizes in hydrated dextran microspheres. Biomacromolecules 1:696–703
Stock SR (1999) X-ray microtomography of materials. Int Mater Rev 44:141–164

Strand BL, Morch YA, Espevik T, Skjak-Braek G (2003) Visualization of alginate-poly-L-lysine-alginate microcapsules by confocal laser scanning microscopy. Biotechnol Bioeng 82:386–394
Sun G, Zhang Z (2001) Mechanical properties of melamine-formaldehyde microcapsules. J Microencapsul 18:593–602
Sun G, Zhang Z (2002) Mechanical strength of microcapsules made of different wall materials. Int J Pharm 242:307–311
Taylor AJ (1998) Physical chemistry of flavour. Int J Food Sci Technol 33:53–62
Teunou E, Fitzpatrick JJ (1999) Effect of relative humidity and temperature on food powder flowability. J Food Eng 42:109–116
Van Raamsdonk JM, Chang PL (2001) Osmotic pressure test: a simple, quantitative method to assess the mechanical stability of alginate microcapsules. J Biomed Mater Res 54:264–271
Verma RK, Krishna DM, Garg S (2002) Formulation aspects in the development of osmotically controlled oral drug delivery systems. J Control Release 79:7–27
Wang C, Cowen C, Zhang Z, Thomas CR (2005) High-speed compression of single alginate microspheres. Chem Eng Sci 60:6649–6657
Weiss G, Knoch A, Laicher A, Stanislaus F, Daniels R (1995) Simple coacervation of hydroxypropyl methylcellulose phthalate (HPMCP). II. Microencapsulation of ibuprofen. Int J Pharm 124:97–105
Westrin BA, Axelsson A, Zacchi G (1994) Diffusion measurements in gels. J Control Release 30:189–199
Xu Y, Du Y (2003) Effect of molecular structure of chitosan on protein delivery properties of chitosan nanoparticles. Int J Pharm 250:215–226
Yadav SK, Khilar KC, Suresh AK (1997) Release rates from semi-crystalline polymer microcapsules formed by interfacial polycondensation. J Memb Sci 125:213–218
Yan NX, Zhang MZ, Ni PH (1992) Size distribution and zeta potential of polyamide microcapsules. J Memb Sci 72:163–169
Yan-yu X, Yun-mei S, Zhi-peng C, Qi-neng P (2006) Preparation of silymarin proliposome: a new way to increase oral bioavailability of silymarin in beagle dogs. Int J Pharm 319:162–168
Yeo Y, Bellas E, Firestone W, Langer R, Kohane DS (2005) Complex coacervates for thermally sensitive controlled release of flavor compounds. J Agric Food Chem 53:7518–7525
Yoshioka Y, Asao K, Yamamoto K, Tachi H (2007) New method for fabricating aromatic polyamide particles with a narrow particle size distribution. Macromol Reaction Eng 1:222–228
Zhang YL, Chu CC (2002) Biodegradable dextran-polylactide hydrogel networks: their swelling, morphology and the controlled release of indomethacin. J Biomed Mater Res 59:318–328
Zhang Z, Ferenczi MA, Lush AC, Thomas CR (1991) A novel micromanipulation technique for measuring the bursting strength of single mammalian-cells. Appl Microbiol Biotechnol 36:208–210
Zhang Z, Ferenczi MA, Thomas CR (1992) A micromanipulation technique with theoretical cell model for determining mechanical properties of single mammalian cells. Chem Eng Sci 47:1347–1354
Zhang Z, Saunders R, Thomas CR (1999) Mechanical strength of single microcapsules determined by a novel micromanipulation technique. J Microencapsul 16:117–124
Zhao L, Zhang Z (2004) Mechanical characterization of biocompatible microspheres and microcapsules by direct compression. Artif Cells Blood Substit Immobil Biotechnol 32:25–40
Zou Y, Brusewitz GH (2002) Flowability of uncompacted marigold powder affected by moisture content. J Food Eng 55:165–171